Acta Technica *61*, No. 4B/2016, 57–74

Numerical analysis and simulation of liquid food temperature fluctuation in an open refrigerated display cabinet

Wensong Lin[1], Tianji Chen[1]

Abstract. Based on the numerical simulation and experimental study on temperature of vertical open refrigerated display cabinets (RDC), some methods of periodic functions and wave shape analysis theory were used for research of the food temperature fluctuation in such a cabinet and temperature fluctuating of chilled liquid food inside RDC was also simulated. The main factors influencing the food temperature fluctuations were analyzed and studied, and the mathematical models of cabinet temperature perturbation and corresponding food temperature response were built; the mathematical models were solved and analyzed by the CFD and wave characteristic functions. The characteristics of food temperature fluctuations were obtained from the results of numerical simulation, and four of them related to liquid foods were compared and analyzed under different on-off ratios and defrost conditions. As the results of simulations show, the temperature fluctuating time of the food with shorter defrost heating time and smaller on-off ratio is shorter and the the height of peak is lower. So, selecting suitable defrosting condition and on-off ratio will optimize the performance of RDC and improve the quality of displayed food.

Key words. Refrigerated display cabinets, food temperature fluctuation, wave shape analysis, numerical simulation, periodic defrost..

1. Introduction

As the terminal equipment of modern food cold chain, open display cabinets are widely used in supermarkets. They can not only guarantee the food quality and freshness, but also have the advantages of good displaying and easy taking the products stored. Compared with the closed display cabinets, the open display cabinets face more problems. The cabinet temperature is, for example, more sensitive to ambient temperature, and a slight temperature rise will cause microbial breeding dangerous to customers. As Schmidt et al. [1] studied, the temperature fluctuation during the defrost period will accelerate the chemical and enzymic changes in the tissue of meat and in dairy products even possibly speed up breeding of microorganism and may cause food spoilage and poisoning. Therefore, the control of RDCs,

[1]Department of refrigeration, Shanghai Ocean University, Shanghai 200090, China

especially their temperature, is very crucial for the chilled food storage industry with rapid development.

The fluctuations of the cabinet temperature are closely related with the characteristics of air supply and defrost of open refrigerated display cabinets. In this field, there is much research on the numerical simulation of the temperature field inside RDC based on computational fluid dynamics (CFD), mainly using the finite difference method, the finite element method, the transformation method, etc., as Cortella et al. [2] summarized. In this paper, based on the numerical simulation and experimental study on temperature characteristic of open vertical refrigerated display cabinets, some methods of periodic function and wave shape analysis theory were used in the research on the food temperature fluctuation. The temperature fluctuating of chilled liquid food inside RDC was simulated, the simulation of food temperature fluctuation was performed considering the disturbance of temperature of air supplied and periodic defrost, which is different from those recommended in literature. The temperature fluctuation of chilled liquid food inside RDC was controlled and suppressed by regulating the wave characteristic of the defrost cycle and on-off ratio of the refrigeration system in order to optimize the performance of RDC and improve the quality of foods on display.

2. Physical model of RDC and liquid food tank

According to the performance test standard of RDC [3], the ambient temperature and humidity was set as 25 °C and 60.0 %. The RDC simulated is an open vertical type with inner and outer dual air curtains, and it has four shelves and bottom display areas as shown in Fig. 1a. The dimension is $2430 \times 1100 \times 1940$ mm, inner volume is 1400 l and total display area is $5.9\,\mathrm{m}^2$. The cabinet temperature range is from -2 °C to 2 °C. Four kinds of liquid food, namely spring water, orange juice, milk, and yoghurt (plain) of same volume (396 ml) were filled fully into four cylindrical containers of same size (60 mm in diameter, 150 mm in height) and same material (paper of thickness 1 mm). The containers were put separately on the same position on the second shelf in RDC (two pieces of insulation material were pasted on the top and bottom of the container for thermal isolation, as shown in Fig. 1b). The influence of RDC horizontal direction was ignored. The standard M packages (oxy-ethyl-methyl-cellulose and water, referring to BS EN441-4 standard [4]) were laid on the other shelves and bottom area in RDC as a regular load in supermarkets.

3. Mathematical model

3.1. Theoretical analysis of numerical simulation

When an open RDC works, Laguerrea et al. [5] found that there is a heat exchange (between foods displayed and air flow inside the cabinet) by heat conduction, convection and radiation all the time. Moreover, food temperature fluctuates with the change in cabinet temperature. There are many factors affecting the change in

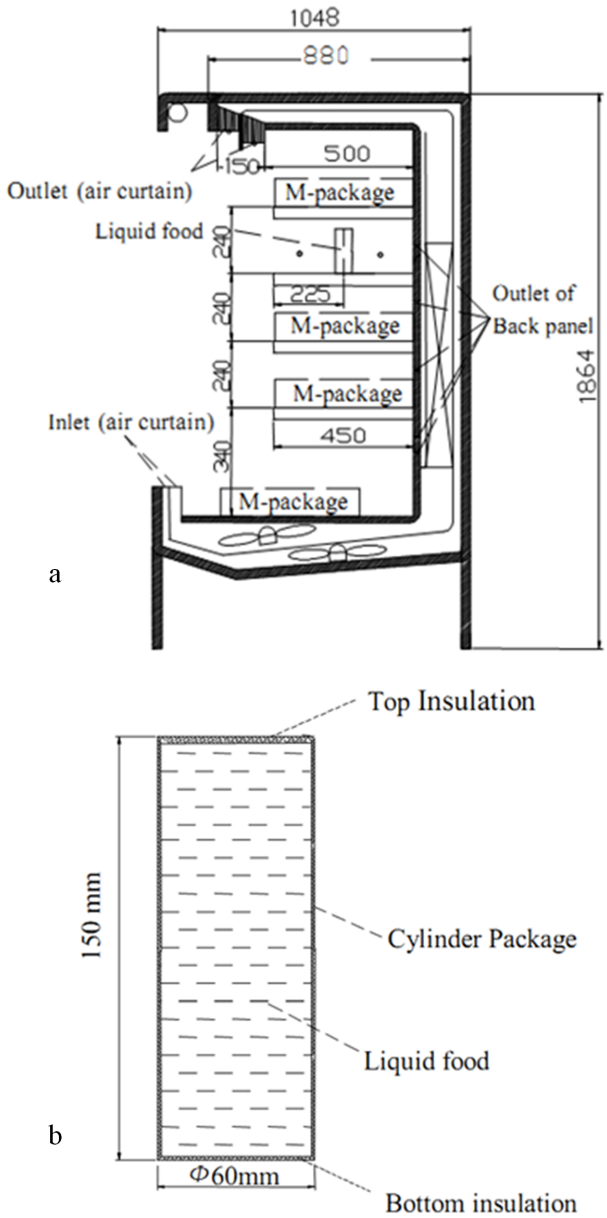

Fig. 1. Layout of tested RDC: a–arrangement (dimensions in mm), b–container with liquid food (dimensions in mm)

cabinet temperature. In general, they are divided into two main parts, periodical ones (the disturbances of temperature of air supplied etc.) and nonperiodical ones (such as the heat load of external air infiltration). The disturbance time of nonpe-

riodical ones is shorter and they are mostly irregular, but the periodical ones occur during the whole operation time of RDC, directly impacting the cabinet temperature. In this paper, three parameters, namely peak height H, fluctuating time λ and delay time t_{h} were used for wave shape analysis. Peak height H means the difference between the maximal and minimal temperatures in a temperature fluctuating cycle (half wave shape), and represents the amplitude of fluctuations. Its value is related to the operation condition of RDC and food category. The time from the start point to the end point of the fluctuating cycle was taken as the fluctuating time λ. It is half wavelength in a defrosting cycle representing the length of defrosting fluctuating time, and becomes full wavelength in a refrigeration cycle, indirectly reflecting the fluctuating frequency and the number of fluctuations. The absolute time different between the time of the peak point in a fluctuating cycle and that of the reference cycle was taken as the delay time t_{h}. It reflects the speed of temperature fluctuating transmission or response, its value is related with the food (package) category and has nothing to do with the operation conditions of RDC.

3.2. The disturbance model of air supply temperature of RDC

3.2.1. The disturbance model of periodic on-off control The start-stop of the refrigeration system and the defrost components are controlled by the control system to maintain the cabinet temperature at the value set. The neutral zone control method is used widely in the control system of RDC. When the cabinet temperature reaches the upper limit set, the controller sends out signals to open the liquid solenoid valve (or impulse electronic expansion valve) and start the compressor, and thus the refrigeration system works and the cabinet temperature decreases. When it reaches the lower limit set, the controller sends out signals again to shut off the liquid solenoid valve and stop the compressor, and thus cabinet temperature rises back. So the on-off control of a refrigeration system is periodic, and the ratio of uptime and downtime is almost constant under the steady operation condition. Thus the air supply temperature fluctuates periodically along with the periodic on-off control. Lazarin and Aprea [6–7] conclude that RDC with different cabinet temperature control system will have different control accuracy of temperature, and especially different on-off time ratio. If R is the on-off time ratio and P is one operation cycle, the uptime of the refrigeration system in one operation cycle is $R \cdot P(1+R)$ and the downtime is $P/(1+R)$. If $t(\tau)$ is the disturbance temperature function caused by on-off control, the periodic impulse τ in one operation cycle P is expressed as

$$t(\tau) = \begin{cases} t_{\mathrm{H}} & 0 < \tau < RP/(1+R) \\ t_{\mathrm{L}} & RP/(1+R) < \tau < P \end{cases}, \tag{1}$$

where t_{H} is the temperature of supplied air when the refrigeration system of RDC starts as the upper limit of cabinet temperature and t_{L} is the temperature of supplied air when the refrigeration system of RDC stops, as the lower limit of cabinet temperature.

By Fourier series expansion, equation (1) becomes

$$t_r(\tau') = \left(\frac{R}{R+1}t_{\mathrm{H}} + \frac{1}{R+1}t_{\mathrm{L}}\right) + \frac{2(t_{\mathrm{H}} - t_{\mathrm{L}})}{\pi}\sin\left(\frac{R}{R+1}\pi\right)\cos\frac{\pi}{P}\tau\,. \qquad (2)$$

3.2.2. The temperature disturbance model of periodic defrost Tasso et al. [8] found that frost forms and accumulates on the evaporator coil surface after a long period of operation, and the heat exchange performance of the evaporator degrades as the frost thickness increases, even blocking the flow passage and resulting in the failure of the compressor by liquid hammer. Therefore, periodic defrost is required to remove the accumulated frost on the evaporator coil in a setting time interval by the control system. When the control system switches to the defrost mode, the refrigeration system stops and the electrical heating runs. When the time or coil temperature reaches the upper limit set, the defrost stops and the cabinet temperature rises to some extent because of the effect of the defrost heating as Lawrence and Evans studied [9]. Because of the periodicity of defrosting process, the air supply temperature changes periodically, and the temperature change caused by defrost can be considered to be an individual disturbance factor. Symbol t_{d} denotes the air supply temperature when defrosting, τ_{d} is the heating time, and τ_{i} is the interval time between two defrosting process, the single defrosting cycle $P' = \tau_{\mathrm{d}}\tau_{\mathrm{i}}$. If $t(\tau')$ is the function of air supply temperature of RDC, the periodic impulse formula is

$$t(\tau') = \begin{cases} t_r & nP' < \tau < nP' + \tau_{\mathrm{i}} \\ t_d & nP' + \tau_{\mathrm{i}} < \tau < (n+1)P' \end{cases} \qquad n = 0, 1, 2, \ldots\,. \qquad (3)$$

In the above formula, t_{r} is the air supply temperature during refrigerated cycle, see equation (2). By Fourier series expansion, the formula (3) becomes

$$t(\tau") = \frac{1}{p'}(t_{\mathrm{r}}\tau_{\mathrm{i}} + t_{\mathrm{d}}\tau_{\mathrm{d}}) + \frac{2(t_{\mathrm{r}} - t_{\mathrm{d}})}{\pi}\sin(\frac{\tau_{\mathrm{i}}}{P'}\pi)\cos\frac{\pi}{P'}\tau\,. \qquad (4)$$

In (4), the defrosting time τ_{d} starts from the timing point when the air supply temperature is over the upper limit of the cabinet temperature t_{H} in the refrigerated cycle. The heating time τ_j generally is set as a fixed value by manual or depends on the time till the coil temperature reaches the fixed value set. When the heating time ends, the air supply temperature reaches the maximum value during the defrosting process, the refrigeration system starts, and the air supply temperature decreases gradually. The time of the defrosting process ends when the air supply temperature reaches the lower limit of the cabinet temperature. In the above process, the air supply temperature changes periodically and can be described as a half-wave sine function with peak of $t_{\mathrm{d,max}} - t_{\mathrm{H}}$ and fluctuating time τ_{d} as shown in Fig. 2.

Its Fourier progression expression is

$$t(\omega\tau'_{\mathrm{d}}) = \frac{t_{\mathrm{d,max}} - t_{\mathrm{H}}}{\pi}(1 + \frac{\pi}{2}\sin\tau_{\mathrm{d}} - \frac{2}{3}\cos 2\omega\tau_{\mathrm{d}}) \quad \text{and} \quad \omega = \frac{1}{2\tau_{\mathrm{d}}}\,. \qquad (5)$$

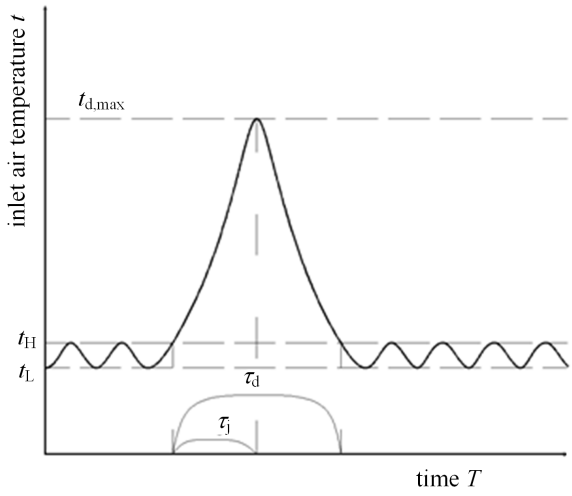

Fig. 2. Graph of half wave sine function of single defrost cycle

Here, quantities $t_{\mathrm{d,max}}$ and τ_{d} are calculated from the formulae

$$t_{\mathrm{d,max}} = t_{\mathrm{H}} + \eta_{\mathrm{e}} W_{\mathrm{e}} \left[\frac{\tau_{\mathrm{j}} - \frac{m_{\mathrm{w}}(C_{\mathrm{p,f}} \Delta T + h_{\mathrm{f}})}{Q_{\mathrm{h}}}}{c_{\mathrm{a1}} m_1} \right], \tag{6}$$

$$\tau_{\mathrm{d}} = \tau_{\mathrm{j}} + \left[\frac{m_1 (h_{1,t_{\mathrm{d,max}}} - h_{1,t_{\mathrm{L}}})}{q_{\mathrm{evp}}} \right]. \tag{7}$$

Here, symbol η_{e} denotes the defrost heating efficiency, W_{e} is the electric heater power in kW, m_{w} stands for mass of defrosting water in kg, $C_{\mathrm{p,f}}$ represents the specific heat capacity of frost in $\mathrm{J\,kg^{-1}\,K^{-1}}$, ΔT is the temperature difference between frost and electric heater in K, h_{f} denotes the fusion enthalpy of frost in J kg−1, Q_{h} represents the heat transfer from electric heater to evaporator in J, c_{a1} stands for specific heat capacity of air, $\mathrm{J\,kg^{-1}\,K^{-1}}$, $h_{1,t_{\mathrm{d,max}}}$ is the enthalpy of air with temperature of $t_{\mathrm{d,max}}$ in $\mathrm{J\,kg^{-1}}$, $h_{1,t_{\mathrm{L}}}$ denotes the enthalpy of air with temperature of t_{L} in $\mathrm{J\,kg^{-1}}$ and, finally, q_{evp} stands for the heat transfer flux from evaporator inside to air in W.

3.3. Simulation and solution of cabinet temperature field

3.3.1. Building of numerical model of temperature field Currently, as D'Agaro [10] concluded, turbulence models are mostly used for mathematical simulation of air curtain and RDC. The mainstream models are $k-\varepsilon$ model, Reynolds Stress Model (RSM) and large eddy simulation (LES) model. In this paper, an improved two-fluid model by Yu [11] is adopted, dividing the air flow into two fluids, the turbulent fluid from air curtain and the non-turbulent fluid outside the cabinet respectively, using the area coefficient of honeycomb as the volume fraction of air through air curtain.

Also a modification of mass transfer rate equation between two fluid is employed to improve the simulation accuracy of cabinet temperature field. In this improved two-fluid model, the food package is assumed as a hermetic cylinder, whose top and bottom are thermally insulated. The two-fluid model for the RDC can be established and the governing transport equations can be written as

$$\frac{\partial}{\partial x_j}(\rho_k r_k U_{kj} \Phi_k) = \frac{\partial}{\partial x_j}(r_k \Gamma_{\Phi k} \frac{\partial \Phi_k}{\partial x_j}) + \frac{\partial}{\partial x_j}(\Phi_k D_{\Phi k} \frac{\partial r_k}{\partial x_j}) + S_{\Phi k} + I_{\Phi k}\,. \qquad (8)$$

Here, the subscript k means the kind of fluid category, which is 1 or 2, the subscript j denotes the space coordinates, symbol Γ_Φ stands for the diffusion coefficient of fluid 1 or fluid 2, D represents the interphase diffusion coefficient between fluid 1 or fluid 2, S is the source term of fluid 1 or fluid 2, I is the interphase source term between fluid 1 and fluid 2, r stands for the volume fraction of fluid, and Φ denotes the dependent variable, corresponding to the continuity equation when taken as 1, momentum equation when taken as velocity, and energy equation when taken as temperature. Finally, ρ_k is the density of fluid k (k being 1 or 2), and U_{kj} is the velocity vector of fluid k (1 or 2) in the spatial y direction.

The disturbance temperature model of air supplied (2) and (4) is employed as the boundary function of the two fluid turbulence model in this paper, and this periodic disturbance boundary function is transferred and imported into user defined functions UDFs with the CFD software FLUENT, then the parameters of two fluids model are set and the computational domain is constructed and meshed for the simulation.

3.3.2. Computational case and grid The parameters of seven cases for simulation of RDC are listed in Table 1 and Table 2.

Table 1. List of input parameters

Parameter	Unit	Value
Ambient temperature T_a	°C	25
Ambient humidity R_a	%	60
Velocity of back air flow v_ba	$\mathrm{m\,s^{-1}}$	0.1
Velocity of outer air curtain* v_oa	$\mathrm{m\,s^{-1}}$	0.25
Velocity of inner air curtain v_{ia}	$\mathrm{m\,s^{-1}}$	0.3
Origin temp. of outer air curtain T_ao0	°C	10
Origin cabinet temperature T_c0	°C	2
Origin food temperature T_f0	°C	10
Food package surface (each side) S_f0	$\mathrm{m^2}$	0.014
Food package thermal conductivity k	$\mathrm{W\,m\,K^{-1}}$	0.9
Inner air curtain/back panel outlet temperature (Refrig. cycle) T_r	°C	$T_\mathrm{r}(\tau)$*
Inner air curtain/back panel outlet temperature (Defrost cycle) T_d	°C	$T_\mathrm{d}(\tau)$*

Note: * Defined temperature boundary function

The temperature change of spring water, orange juice, milk and yoghurt is investigated from case 1 to case 7, respectively. The initial temperature of the inner and outer air curtains is based on the experimental data for a better comparison. Thermophysical parameters of four liquid food samples are shown in Table 3 [12–16]. Neutral zone control is used for cabinet temperature control, and the initial cabinet temperature is set to be 2 °C. The on-off time ratio of the refrigerated system, defrost heating time and other parameters are shown in Table 2.

Table 2. Computational cases

Case	On-off ratio R	Defrost conditions	
No.	(-)	Heating time τ_d (min)	Interval time τ_i (min)
1	0.65	20	180
2	0.65	25	240
3	0.65	30	300
4	0.55	20	180
5	0.6	20	180
6	0.7	20	180
7	0.75	20	180

Table 3. Thermophysical properties parameters of liquid food samples [12–16]

Liquid food	Density ϱ ($\mathrm{kg\,dm^{-3}}$)	Specific heat capacity C ($\mathrm{kJ\,kg^{-1}\,K^{-1}}$)	Therm. conductivity k ($\mathrm{W\,m^{-1}\,K^{-1}}$)
Spring water	1.00	4.18	0.58
Orange juice	1.01	3.73	0.55
Milk	1.03	3.77	0.50
Yoghurt (plain)	1.05	3.52	0.48

As shown in Fig. 3, some parts or area of RDC as the evaporator, insulation layer and the propeller fan are removed in order to simplify the simulation. Considering that the open boundary conditions of the display cabinet are uncertain, the computational domain is extended until the effect of the display cabinet opening is negligible there. Then the computational domain becomes a irregular region of dimensions 1.07 m×1.41 m and the asymmetric grid consists of 44×36 cells, which were generated to mesh the computational domain. A denser grid is adopted in the air curtain inlet and outlet, back panel air outlet and surround of liquid food regions where the air flow is complex. For simplification of simulation, the plates of shelves are assumed to be insulated, see the details in Fig. 3, upper and bottom parts.

3.4. Response model of food temperature fluctuation

The heat transfer between the liquid food and airflow inside the cabinet occurs mainly by heat convection, and the cabinet temperature fluctuation gradually transfers into the interior of liquid food and causes the temperature fluctuated periodically

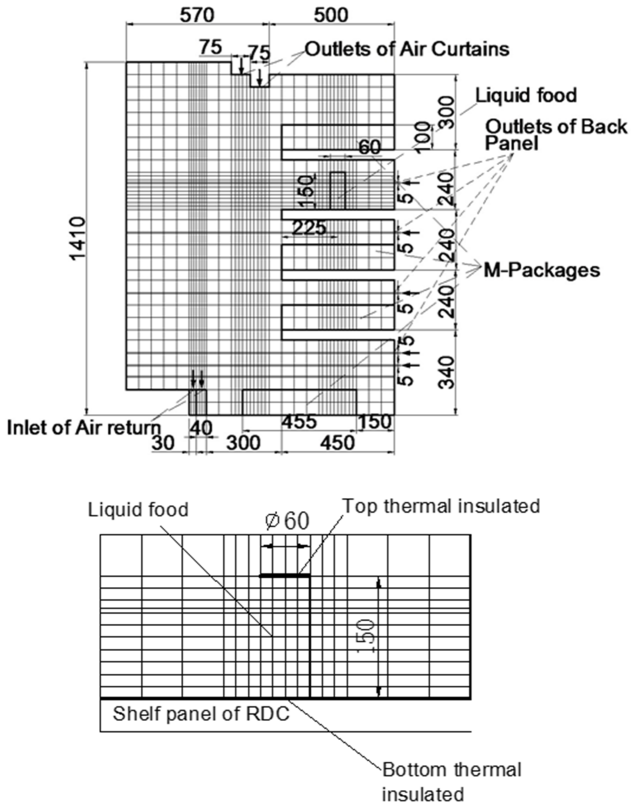

Fig. 3. Computational domain and grid of cabinet and liquid food: up–computing zone of RDC, bottom–computing zone around liquid food

with it. The food package is assumed as a hermetic cylinder with dry surfaces and insulated at top and bottom, so there is no mass transfer and the radiation is negligible. There is only convection between food package wall and airflow surrounded. A cylindrical coordinate system is built based on the structure of package, and a none-dimensional unsteady-state heat transfer model is established based on these assumptions and simplification. The instantaneous average temperature of 11 cells adjacent the wall of package on left and right sides (as shown in Fig. 3 bottom part) is used as the boundary air temperature in the calculation of this model, and the parameters related are set referring to the following equations [12–15].

According to the assumptions, the energy equation of liquid food is

$$\rho C_{\mathrm{p}} \frac{\partial T}{\partial t} = \frac{m}{r} k \frac{\partial T}{\partial r} + \frac{\partial k}{\partial r} \frac{\partial T}{\partial r} + k \frac{\partial^2 T}{\partial r^2} \,. \tag{9}$$

The mass equation has the form

$$\frac{\partial V}{\partial t} = \frac{m}{r} D \frac{\partial V}{\partial r} + \frac{\partial D}{\partial r} \frac{\partial V}{\partial r} + D \frac{\partial^2 V}{\partial r^2} \,. \tag{10}$$

The boundary condition between the food package and air is is given by the formula

$$-k\left[\frac{\partial T}{\partial r}\right]_{r=r_0} = \alpha F\left[T_{\mathrm{s}}(\tau,r) - \overline{T}_{\mathrm{air}}(\tau)\right] . \tag{11}$$

Here, $\overline{T}_{\mathrm{air}}(\tau)$ means the instantaneous average temperature of 11 cells adjacent the wall of package on both left and right sides.

The heat transfer equation between the liquid food and the food package is described by the formula

$$-k\left[\frac{\partial T}{\partial r}\right]_{r=r_1} = \omega\left[T_{\mathrm{s}}^{'}(\tau) - T_{\mathrm{i}}(\tau,r)\right] , \tag{12}$$

where $T_s^{'}(\tau)$ means the temperature of the inner surface of the package, and $T_i(\tau,r)$ denotes the temperature of the liquid food inside.

4. Results and discussion

4.1. Numerical simulation results of cabinet temperature fluctuation

The temperature field of the cabinet during the refrigeration cycle and the defrost cycle were simulated, respectively, as shown in Figs. 4 and 5. Figure 5 shows the distribution of temperature field at some point during the refrigeration cycle. From the figure, it can be seen that the distribution of the temperature field in each shelf has a certain difference, resulting in different distribution of temperature with M packages. The average temperatures in the 2nd and 3rd shelf are lower than those in other three shelves and the temperature of M packages in the 3rd shelf is also lower than those in other shelves. The significant temperature stratification is found inside the liquid food with package, and the temperature is high when the position is closer to the center of package.

Figure 5 shows the distribution of the temperature field at some point during the defrost cycle. From Fig. 5, it can be seen that the temperature distribution in each shelf is more uniform, and the distribution temperature of M packages in each shelf is very close, and the significant temperature stratification is also found inside the liquid food. The temperature is lower when the position is closer to center of the package.

4.2. Feature analysis of food temperature fluctuating response at different positions

The fluctuating response of the food temperature (in defrost cycles) in the cabinet in case 1 was calculated. The wave shape of average temperature curve in 2nd shelf was calculated and used as a reference wave shape, and then the characteristic numbers of temperature curve of different liquid food were calculated and analyzed basing on this reference wave shape. Figure 6 show the change in fluctuating char-

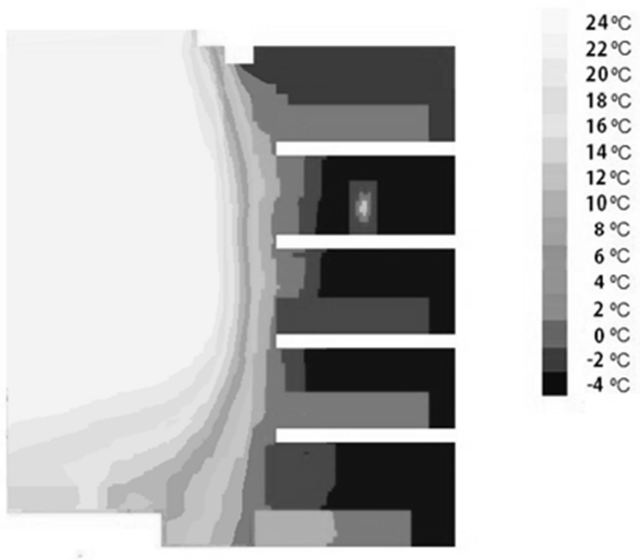

Fig. 4. Simulation of cabinet temperature field in refrigeration cycle (case 1)

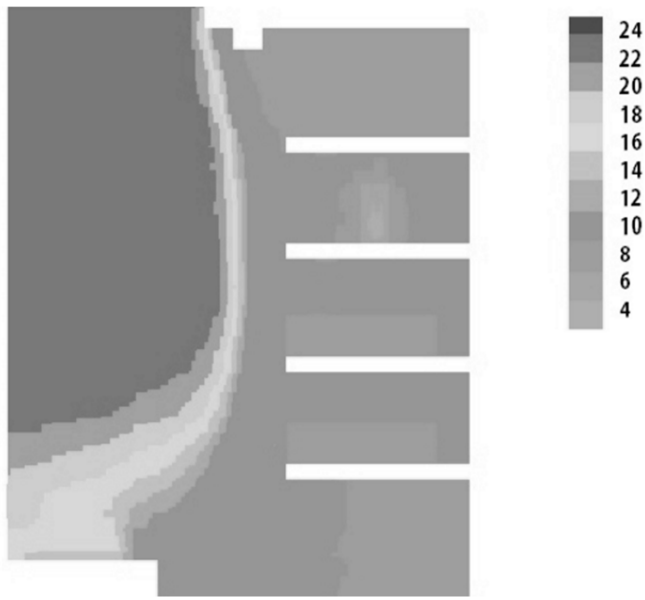

Fig. 5. Simulation of cabinet temperature field in defrost cycle (case 1)

acteristic numbers at different positions from outside to the center of the liquid food.

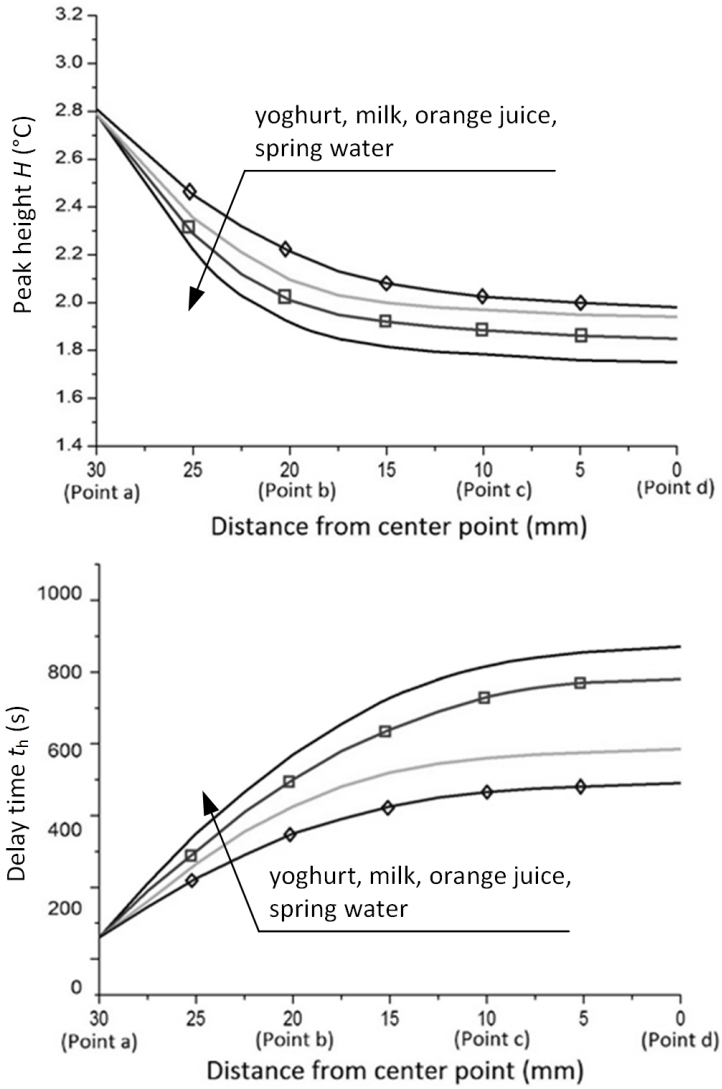

Fig. 6. Change in fluctuating characteristic numbers at different positions from outside to the center of the liquid food: up–peak height of each liquid food at different position, bottom–delay time of each liquid food at different position

It can be seen from Fig. 6 that some fluctuating characteristics of inner temperature of each liquid food correspond with the fluctuation of the cabinet temperature. The change of fluctuating characteristic of each liquid food from the outer points to inner points shows the obvious trend as follows: the peak height of temperature wave on the surface of each liquid food is higher around 2.8 °C, and drops gradually from the surface to center. On the contrary, the delay time of each liquid food increases. Taking spring water as an example, the peak height decreases by 1.04 °C

and delay time t_h increases 14.5 times. Furthermore, the fluctuating characteristic numbers of each liquid food shows a drastic change in the first 10 mm from outside (from the point a to point b), and gradually flattens in the final interval (from the point b to point d), such as the peak height of spring water decreases sharply by almost 1 °C (from 2.8 °C to 1.86 °C) in the first 10 mm and then decreases slightly by 0.1 °C (from 1.86 °C to 1.76 °C) in the final 20 mm. The delay time of spring water increases sharply almost 10 times (from 60 s to 590 s) in the first 10 mm and then it increases slightly 1.5 times (from 590 s to 87 s) in the final 20 mm.

4.3. Influence of different on-off ratio on food temperature fluctuating

The change in fluctuating characteristic numbers at the center of each liquid food was simulated and calculated with different on-off ratio R from 0.55 to 0.75 (case 1, 4–7), and the results are shown in Fig. 7.

From Fig. 7, it can be seen that the peak height of each liquid food changes from 0.14 °C to 0.22 °C, and also increases to some extent, by 25.4 %, 25.6 %, 26.4 % and 28.6 % for spring water, orange juice, milk, and yoghurt, respectively. The fluctuating time of each liquid food during one single refrigeration cycle changes between 160 s to 195 s, and increases to some extent with an increase of the on-off ratio from 0.55 to 0.75 by 11.1 % for spring water, 12.8 % for orange juice, 14.9 % for milk, and 15.5 % for yoghurt, respectively. As the calculations show, when on-off ratio R of RDC is smaller, the on-off frequency is higher and the interval time between run and stop is shorter, then the fluctuating time λ and peak height H of temperature fluctuating inside food is shorter accordingly. Vice versa, when on-off ratio R is higher, the on-off frequency is lower and the interval time between run and stop is longer, then the fluctuating time λ and peak height H of temperature fluctuating inside food will be longer and higher accordingly. The calculations also show that the peak height of each liquid food at center position is shorter and between 0.14 °C to 0.22 °C with the change of R, but considering the temperature fluctuation is of high frequency (about 3 min per cycle) and long time (3–5 hours), its impact on food quality cannot be ignored, either.

4.4. Influence of different defrost condition on food temperature fluctuating

The simulation shows that the fluctuating characteristic of cabinet temperature is different under different defrost conditions and results in different fluctuating of liquid food temperature. The peak height of the average temperature fluctuating in the second shelf in three defrost cases (1–3) is listed in Table 4.

The temperature change at the center of four kinds of liquid food in three defrost cases was simulated, and the changes in peak height H and fluctuating time λ obtained by the method of the wave shape characteristic analysis are shown in Fig. 8.

From Fig. 8, it can be seen that the range of peak height H of each liquid food at the center point is between 1.8 °C to 2.3 °C and the range of fluctuating time λ is between 7500 s to 8600 s. In all the considered cases, with the increase of defrost

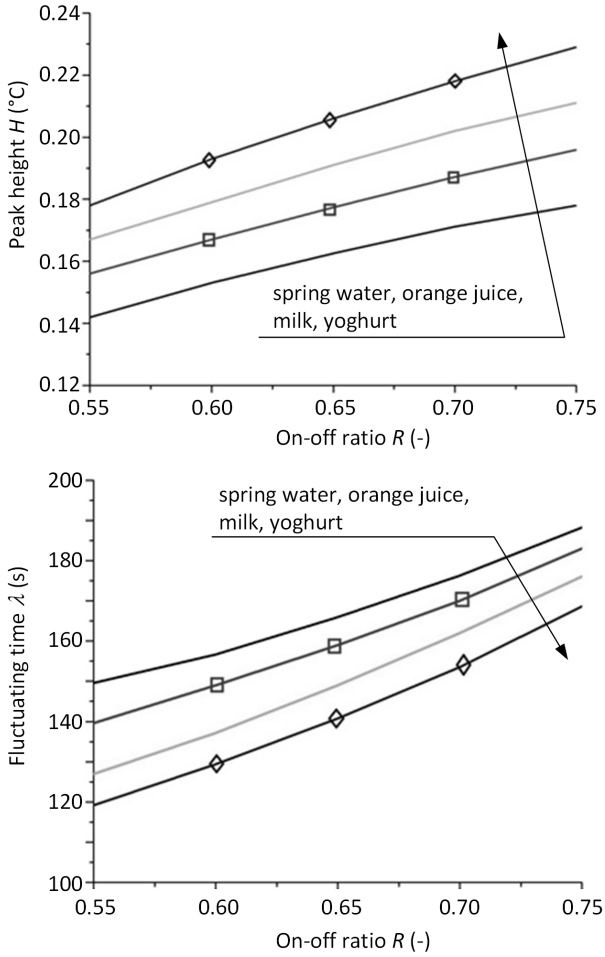

Fig. 7. Change in fluctuating characteristic numbers at center point of the liquid food with different on-off ratios R: up–peak height of considered liquid food with different on-off ratios, bottom–fluctuating time of considered liquid food with different on-off ratio

heating time and interval time, the fluctuating time in spring water during one single defrost cycle increases by 3.7 % and the peak height increases by 0.28 °C, the fluctuating time in orange juice increases by 5.1 % and the peak height increases by 0.31K; the fluctuating time in milk increases by 6.9% and the peak height increases by 0.33 °C, and finally, the fluctuating time in yoghurt increases by 8.1 % and the peak height increases by 0.35 °C. Thus, with the increases in the defrost interval time and heating time, the fluctuating time λ of each liquid food at the center point increases by 3.7 %–8.1 %, and peak height H also increases by 0.28–0.35 °C. It is likely that, in a certain range, if the defrosting interval time of RDC is shorter, the heating time will be also shorter and the temperature fluctuating will be smaller.

Thus, there will be more benefits to improve the quality of chilled food displayed.

Table 4. Peak height change of shelf temperature with various RDC defrosting cycle

Case	Interval time τ_{i} (min)	Heating time τ_{j} (min)	Average peak of second shelf temperature $\overline{T}_{\mathrm{air}}$ (°C)
1	3	20	9.25
2	4	25	10.85
3	5	30	12.35

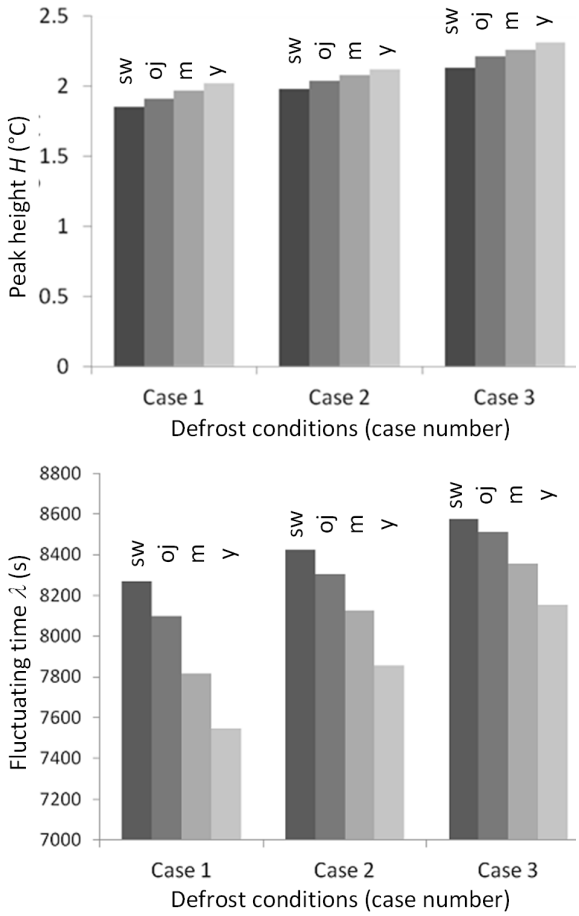

Fig. 8. Change in fluctuating characteristic numbers at center point of the liquid food with different defrost conditions: up–peak height of each liquid food in different defrost cases, bottom–fluctuating time of each liquid food with different defrost cases (sw-spring water, oj–orange juice, m–milk, y–yoghurt)

5. Conclusions

1. As theories and experiment indicated, periodic on-off control of refrigeration system and defrosting are two major interfering factors caused the temperature fluctuation in RDC, and different on-off ratio and defrosting conditions will cause different degrees of temperature rise and fluctuating.

2. A mathematic model of the temperature fluctuations inside the RDC and a fluctuating response model of food temperature corresponded have been built, and the disturbance temperature model of air supplied and periodic defrost has been employed to be the initial condition. The temperature field in RDC and the fluctuating characteristic of the liquid displayed have been simulated and calculated.

3. The temperature fluctuating characteristics of four liquid foods in RDC under refrigeration cycle and defrost cycle were simulated and calculated respectively. The results show that: under defrost cycle (case 1), the peak height of surface temperature wave of each liquid food is around 3 °C, and it decreases gradually from the surface to center. First, at 10 mm distance from the surface, the peak height decreases obviously from 3 °C to 2 °C, but it keeps around 2 °C with only a tiny change in the remaining 20 mm distance to the center. Under refrigeration cycle, the peak height of each liquid food at center position is shorter around 0.2 °C, but considering the temperature fluctuation of higher frequency (about 3 min per cycle) and long time (3–5 hours), its impact on food quality cannot be ignored.

4. As simulation results shown, when on-off ratio R of RDC is smaller, the on-off frequency is higher, the interval time between run and stop is shorter and fluctuating frequency of temperature inside food is relatively higher. Then the time λ and peak height H of temperature fluctuating inside food will be shorter accordingly. Conversely, when on-off ratio R is higher, the on-off frequency is lower, the interval time between run and stop is relatively longer, and the fluctuating frequency is lower. Then the time and peak height of temperature fluctuating inside food will be longer and higher accordingly. Such as, in a single refrigeration cycle, the fluctuating time of each liquid food increased by 11.1–15.5 % and peak height increased by 23.6–28.6 % with on-off ratio increased from 0.55 to 0.75.

5. This study shows that with the increase of defrosting interval time and heating time, the fluctuating time λ of each liquid food at center position increases by 3.7%–8.1%, and the peak height H also increased by 0.28–0.35K accordingly. So, in a certain range, if the defrosting interval time of RDC is shorter, the heating time will be shorter and the temperature fluctuating will be smaller, there will be more beneficial to improving the quality of chilled food displayed.

References

[1] V. J. S. Schmidt, V. Kaufmann, U. Kulozik, S. Scherer, M. Wenning: *Microbial biodiversity, quality and shelf life of micro filtered and pasteurized extended shelf life (ESL) milk from Germany, Austria and Switzerland.* IJ Food Microbiology *154* (2012), Nos. 1–2, 1–9.

[2] G. Cortella, M. Manzan, G. Comini: *CFD simulation of refrigerated display cabinets original research article.* IJ Refrigeration. *24* (2001), No. 3, 250–260.

[3] *ASHRAE Standard 72/1998, Methods of testing open refrigerators.* American Society of Heating, Refrigerating and Air-Conditioning Engineers, Inc., Atlanta, 1998.

[4] *British Standard BS EN441-4: Refrigerated display cabinet, part 4*, 1995.

[5] O. Laguerre, M. H. Hoang, V. Osswald, D. Flick: *Experimental study of heat transfer and air flow in a refrigerated display cabinet.* J Food Eng. *113* (2012), No. 2, 310–321.

[6] R. Lazzarin, M. Noro: *Experimental comparison of electronic and thermostatic expansion valves performance in an air conditioning plant.* IJ Refrigeration *31* (2008), No. 1, 113–118.

[7] C. Aprea, R. Mastrullo, C. Renno: *Performance of thermostatic and electronic expansion valves controlling the compressor.* IJ Energy Research. *30* (2006), No. 15, 1313–1322.

[8] S. A. Tassou, D. Datta: *Influence of supermarket environmental parameters on the frosting and defrosting of vertical multi-deck display cabinets.* ASHRAE Transactions *105* (1999), No. 2, 491–496.

[9] J. M. W. Lawrence, J. A. Evans: *Refrigerant flow instability as a means to predict the need for defrosting the evaporator in a retail display freezer cabinet.* IJ Refrigeration *31* (2008), No. 1, 107–112.

[10] P. D'Agaro, G. Cortella, G. Croce : *Two- and three-dimensional CFD applied to vertical display cabinets simulation.* IJ Refrigeration *29* (2006), No. 2, 178–190.

[11] Yu Ke-zhi, Ding Guo-liang, Chen Tian-ji: *Modified two-fluid model for air curtains in open vertical display cabinets.* IJ Refrigeration *31* (2008), No. 3, 472–482.

[12] S. Peacock: *Predicting physical properties of factory juices and syrups.* International Sugar Journal *97* (1995), No. 1163, 571–572 and 575–577.

[13] R. Ibarz, V. Falguera, A. Garvin, S. Garza, J. Pagan, A. Ibarz: *Flow behavior of clarified orange juice at low temperatures.* J Texture Studies *40* (2009), No. 4, 445 to 456.

[14] I. M. Afonso, L. Hes, J. M. Maia, L. F. Melo: *Heat transfer and rheology of stirred yoghurt during cooling in plate heat exchangers.* J Food Eng. *57* (2003), No. 2, 179–187.

[15] I. H. Tavman, S. Tavman: *Measurement of thermal conductivity of dairy products.* J Food Eng. *41* (1999), No. 2, 109–114.

[16] R. Coquard, B. Panel: *Adaptation of the FLASH method to the measurement of the thermal conductivity of liquids or pasty materials.* IJ Thermal Sciences *48* (2008), No. 4, 747–760.

Received November 16, 2016